Physical Model of Vertical Water Movement Inside a Soil-Column Apparatus for Infiltration Study with A Two-Way Orientation Approach

Reza Adhi Fajar[1], Gunawan Handayani[2], Lilik Eko Widodo[3,*], Sudarto Notosiswoyo[3] & Tri Chandra Pamungkas[4]

[1]Post Graduate Program in Mining Engineering, Faculty of Mining and Petroleum Engineering, Institut Teknologi Bandung, Jalan Ganesha No.10, Bandung 40132, Indonesia
[2]Earth Physics and Complex-system Research Group, Faculty of Mining and Petroleum Engineering, Institut Teknologi Bandung, Jalan Ganesha No.10, Bandung 40132, Indonesia
[3]Earth Resources Exploration Research Group, Faculty of Mining and Petroleum Engineering, Institut Teknologi Bandung, Jalan Ganesha No.10, Bandung 40132, Indonesia
[4]Microelectronics Centre, Inter-University Centre, Institut Teknologi Bandung, Jalan Ganesha No.10, Bandung 40132, Indonesia
*E-mail: lew@mining.itb.ac.id

Abstract. To improve the theory of Richard's equation, studying infiltration under free-draining conditions at the ground surface is necessary. Verification is required to clarify the physical model of water movement. The aim of this study was to describe multistage measurements of both the wetting and the drying front scheme of one-dimensional infiltration at laboratory scale. A soil-column infiltration apparatus was built consisting of a double acrylic wall, a sensor set and a light bulb. Acrylic was chosen as the material for the wall to minimize possible heat conduction on the wall side, which was wrapped in double insulation to achieve adiabatic condition. The following three main sensors were used and controlled by a microcontroller: water-content, pressure and temperature sensors. Meanwhile, the light bulb at the top of the apparatus was set to non-isothermal condition. The instrument was successfully built to describe vertical water movement. Slight modifications were carried out to ensure more precise observation. This resulted in the initiating of new shape interpretation based on the water-ponding measurement to refine the simplified pattern that was introduced by the conventional Green-Ampt theory.

Keywords: *adiabatic; infiltration; non-isothermal; soil-column; water-ponding.*

1 Introduction

Illustrating groundwater movement in terms of hydrology for the vadose zone usually only involves mass conservation through the aspect of the hydraulic gradient. The phenomenon of water movement is caused by gravity, which is

Received October 29th, 2019, 1st Revision March 5th, 2019, 2nd Revision May 20th, 2019, 3rd Revision June 21st, 2019, Accepted for publication August 16th, 2019.
 ISSN: 2337-5779, DOI: 10.5614/j.eng.technol.sci.2019.51.5.2

then considered to be the only driving force in the form of the hydraulic gradient [1-5]. However, some water components in the vapor phase return to the surface at minimum rainfall conditions in long dry periods, so it can be assumed that not all water moving down during infiltration will entirely become groundwater recharge [1,6,7]. In such cases there is a miscalculation in the determination of the volume of water infiltration that becomes groundwater recharge because of ignoring the thermal aspect of the infiltration phenomenon. This study tried to incorporate evaporation with consideration of a second driving force in the form of the thermal gradient caused by the propagation of heat in the vadose zone, which in turn causes some of the water to transform into steam and return to the surface.

The Green-Ampt theory [8] conveniently outlines a simplified water-ponding model to describe the infiltration process in the vadose zone above groundwater level. The downward movement of water is often modeled using the mass movement of piston-patterned water with a downward orientation of the wetting front. Furthermore, modified versions of the Green-Ampt theory have been proposed by subsequent researchers to improve the water-ponding model of downward infiltration in the form of the water content distribution [3,9-18]. The model of water movement at the ground surface is usually simplified in the form of a soil-column apparatus as a physical model at laboratory scale, based on the first driving force. The usage of similar apparatuses has been demonstrated by researchers to reconstruct the downward infiltration model as well [5,19-23]. These apparatuses were used as a physical model of the infiltration process without the involvement of heat conduction as a second driving force. Meanwhile, there has been less research on upward evaporation models incorporating the interference of downward water flux [1,6,24-29]. Several other experiments regarding the same apparatus have been specifically done for the upward-evaporation model based on the second driving force [30,31].

It is necessary to reach a more comprehensive improvement of the water movement formulation to reduce the miscalculation of the volume of groundwater recharge. Therefore, the wetting front shape in the abovementioned preview studies needs to be corrected with the consideration of heat in the infiltration process. Modification of the soil column apparatus is needed to represent the driving force from heat conduction for the movement of water during infiltration under free-draining conditions [7]. The new water-ponding model that emerges is a superposition of the two models. The evaporation process is seen as the opposite of the infiltration process, so that the upward mass movement of steam (water) is modeled using the mass movement of piston-patterned water with an upward drying front. If these two opposite orientations are examined in parallel, the concept of the water-movement model

under free-draining conditions can be established. This research describes multistage measurements of the 1D infiltration process at laboratory scale to obtain a comprehensive view of both the wetting and the drying front schemes in parallel. This was done to compare the pattern of water-ponding during conventional infiltration and during infiltration under free-draining conditions at laboratory scale with non-isothermal and non-adiabatic conditions.

2 Material and Methods

2.1 Conceptual Model

The description of the conventional infiltration process is based on Darcy-Buckingham's law of unsteady groundwater movement in unsaturated soil that is part of the vadose zone. Darcy-Buckingham's law applied to groundwater equations or Richard's equation [8] is only based on mass conservation by describing the phenomenon of infiltration as isothermal and under adiabatic conditions. A simplified solution of Richard's equation can be approached by the Green-Ampt theory. This theory represents the movement of the wetting front shape in the form of the water-content distribution in the vertical direction, while the wetting front is stated as the midpoint of the wetting zone in terms of depth [4,22]. The one-dimensional (1-D) schematic movements are symbolized by water content (θ) and depth (z) (Figure 1).

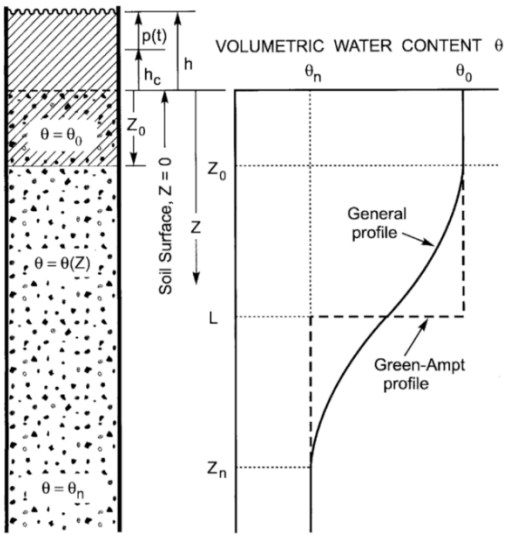

(a) Diagram of ponded water (b) Water-content profiles

Figure 1 Simplified piston water-ponding model based on Green Ampt theory [15].

A conceptual model was constructed, followed by physical modeling in the form of laboratory testing by simulation of the infiltration and evaporation phenomena in soil samples in a soil-column apparatus. The physical model in question is an infiltration column in the form of a soil column used to simulated 1D water displacement with variation of heat and discharge of water flow in the soil. Work on the infiltration column, sensor configuration, and experimental preparation was carried out to obtain a water-ponding model from the series of experiments that simulates a gradual infiltration process. Each trial series illustrated the water-ponding pattern for the three conditions of groundwater displacement as shown in Figure 2.

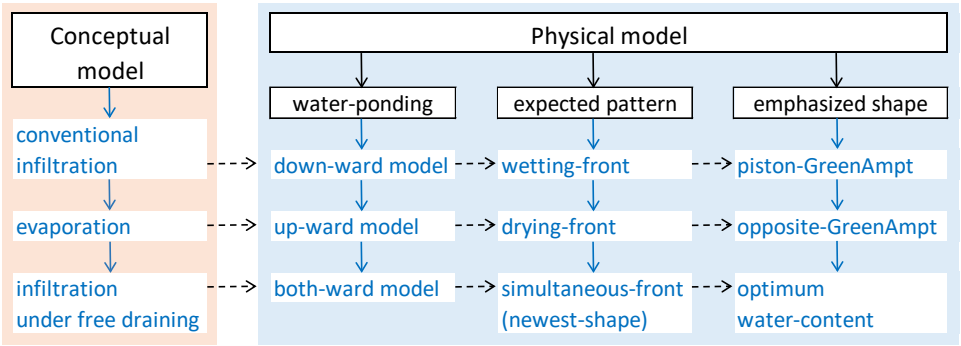

Figure 2 Experimental framework.

2.2 Apparatus Setup

Multistage measurements were executed in the soil-column apparatus. The main parts of the apparatus were: transparent walls, a steel cornerstone, a pipe for intake-outtake water, a sensor set, and a light bulb. The apparatus was adjusted to model a 1D infiltration and evaporation scheme in the same observation tube. A schematic of the soil-column infiltration apparatus is shown in Figure 3.

The acrylic wall had a height of 100 cm. The soil sample was placed at a height of 50 cm. The scale-up criterion or the principle of 1D straight/upright in the theory of uncertainty was adopted through the thickness of the porous media inside the apparatus.

Acrylic was chosen as the material for the wall to minimize possible heat conduction along the wall and was wrapped in double insulation (i.e. 15 cm for the inner wall and 25 cm for the outer wall for adiabatic conditions). The sensors (Figure 4) were assembled on a mobile stick at the center of the apparatus. They were installed in parallel at heights of 5 cm, 20 cm, 35 cm and 45 cm from the bottom. Meanwhile, the light bulb was placed at the top of the apparatus as a miniature sun to create non-isothermal condition.

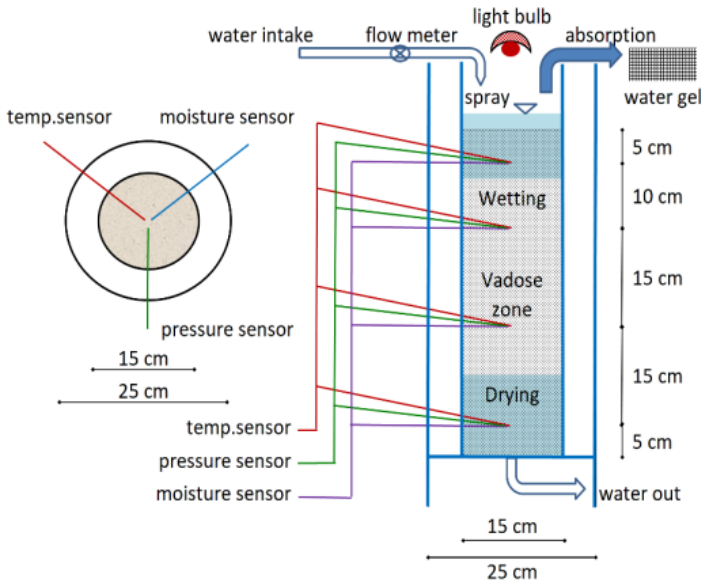

Figure 3 Schematic infiltration process experiment.

2.3 Sensor Configuration

The following three main sensors were installed and observed in parallel: (i) soil-moisture sensor, (ii) pressure sensor, and (iii) temperature sensor (Figure 4).

The soil-moisture sensor measured the water content from the liquid side of the fluid and the pressure sensor measured the air pressure trapped in the porous media. A pressure tube was installed to avoid direct contact between the liquid and the pressure sensor. There are two types of moisture sensors: a resistance-based sensor and a capacitance-based sensor. The resistance-based soil moisture sensor spreads the electricity between two separate plates for interpreting the moisture level [32]. The capacitance-based soil moisture sensor uses the parallel-plate capacitor concept for measuring the soil capacitance, which is directly proportional to the moisture level [33,34].

Table 1 Sensor properties.

Sensor	Measured	Range	Read	Accuracy
LM35	Temperature	0 - 100°C	0.01	0.5°C
SM	Water content	0 - 0.5	0.001	0.05
DFROBOT SM v.1	Water content	0 - 0.5	0.001	0.05
Omron 2SMPP-03	Pressure	0 - 50 kPa	0.01	0.5
Waterflow	Debit	-	0.01	0.5 ml

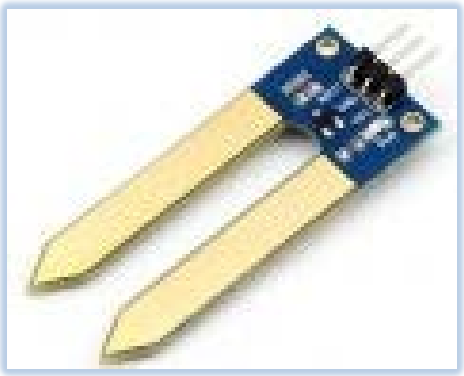

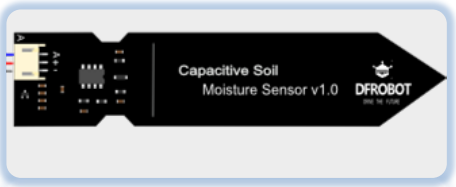

(a) Soil-moisture sensor: Resistance-based (left), Capacitance-based (right)

(b) Pressure sensor

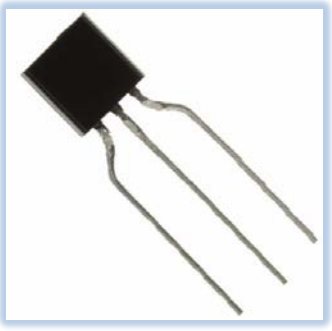

(c) Temperature sensor

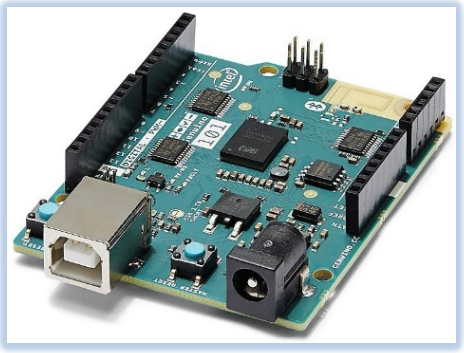

(d) Microcontroller

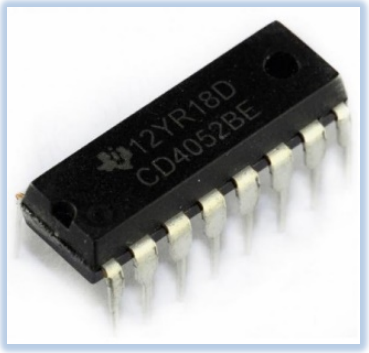

(e) Multiplexer

Figure 4 Electronic components.

Data collection from these sensors was processed using an Arduino 101 microcontroller (Arduino-Genuino-101-3) with 16 analogue and digital pins (Figure 4(d)). Subsequently, a multiplexer (CD4052 type) was used to collect the signal by analogue pins (Figure 4(e)). A multiplexer was needed to combine the sensors signals into one single output. This implementation allowed the

circuit to use only one output pin for each type of sensor. A low *on* impedance and a very low *off* leakage current were used to measure the analogue multiplexer [35,36], as shown in Figure 5.

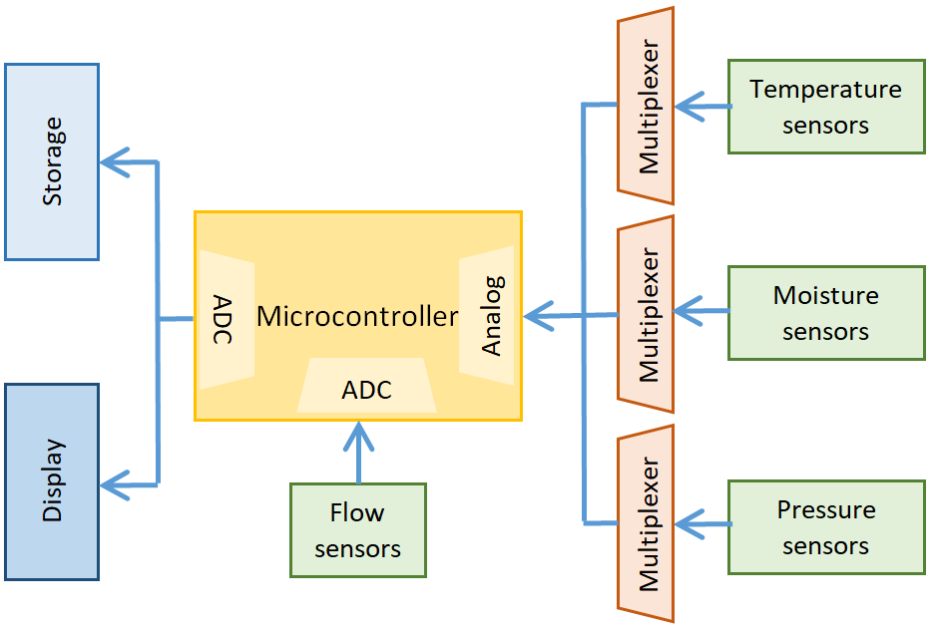

Figure 5 Schematic of data processing.

2.4 Experimental Preparation

Certain procedures are necessary to guarantee a high-quality preparation of (i) the porous media, and (ii) the liquid to be inserted. We used silica sand soil and pure water without any organic compounds.

The soil size was equal to 30-60 mesh (grain-size category of the American Association of State Highway and Transportation Official soil classification system). The water was processed using a purification technique to ensure that it was free from heavy metals, such as metal ions inside the molecules, i.e. in crystal-like form.

The aim of the usage of porous media and liquid fluid was to avoid the possibility of a chemical reaction to achieve the physical approach. Furthermore, a couple of pre-test experiments were prepared to ensure the apparatus quality, including leakage test of the water pressure, sensor reading and adiabatic wall testing (Figure 6).

(a) Water-pressure leakage test

(b) Sensor-reading test

(c) Adiabatic wall test

Figure 6 Pretesting experiments.

3 Results and Discussion

3.1 Experimental Sequels

Three phenomena were simulated with the experimental apparatus in sequel, for the following water movement directions: (i) downward, (ii) upward, and (iii) both directions. The experiments were basically a simple miniature of the processes of isothermal infiltration, non-isothermal evaporation, and infiltration under free-draining conditions. The first experiment was done to exemplify the Green-Ampt theory through the porous media material of silica sand soil. The second experiment was conducted to prove the water-loss phenomenon as the opposite of the Richard equation solution in the vadose zone. The third experiment combined the two previous sequels in view of the initiation of a new shape interpretation based on water-ponding measurements under a non-isothermal infiltration process.

The water movement directions were applied by conditioning the upper flux with different treatments for each experimental sequel. There was no intake or outtake water from the bottom of the apparatus. The first experiment was performed with dry soil conditions under water dropping from the top. The second experiment was conducted with saturated soil conditions under heat flux using the light bulb. The third experiment was conducted with residual water-content conditions of the soil under water dropping and heat flux. Prior to the experiments, the soil material was settled inside the apparatus for at least 1 day to avoid unnecessary data fluctuation from sensor readings because of the soil replacement process [37].

Table 2 Movement rate in units of water drops.

Orientation	Water drop*	Water-loss prediction**	Duration	Remark
Downward	25/min	-	1047 s	Fully saturated
Upward	-	38.3 ml/h	230.5 h	Fully dry
Both-ward	0.5/min	38.3 ml/h	230.5 h	Moisture

*) 1 drop = 0.05 ml

**) water-loss = soil volume / duration

Water flux was dropped from the top of the apparatus at 8.33 ml/s and 0.167 ml/s for the first and third sequels, respectively. No water dropping was applied during the second experiment (Table 2). The units used in the simulation were water drops, assuming a density of 1 g/ml. One drop should have an average volume of 0.05 ml. For the experiments, the amount of liquid absorbed by the porous media was predicted up to 8831 ml based on the volume of the apparatus. The experimentation time was adjusted and specified by the

completion of saturation and fully dry conditions in the first and second experiments, respectively. Meanwhile, the elapsed time of the measurement activity in the third experiment was matched to that of the second one.

3.2 Water-Movement Patterns

The measurement results from the experiments are shown as soil moisture and pressure variations. The water movement of the materials was measured and identified as wetting, drying and simultaneous front curves.

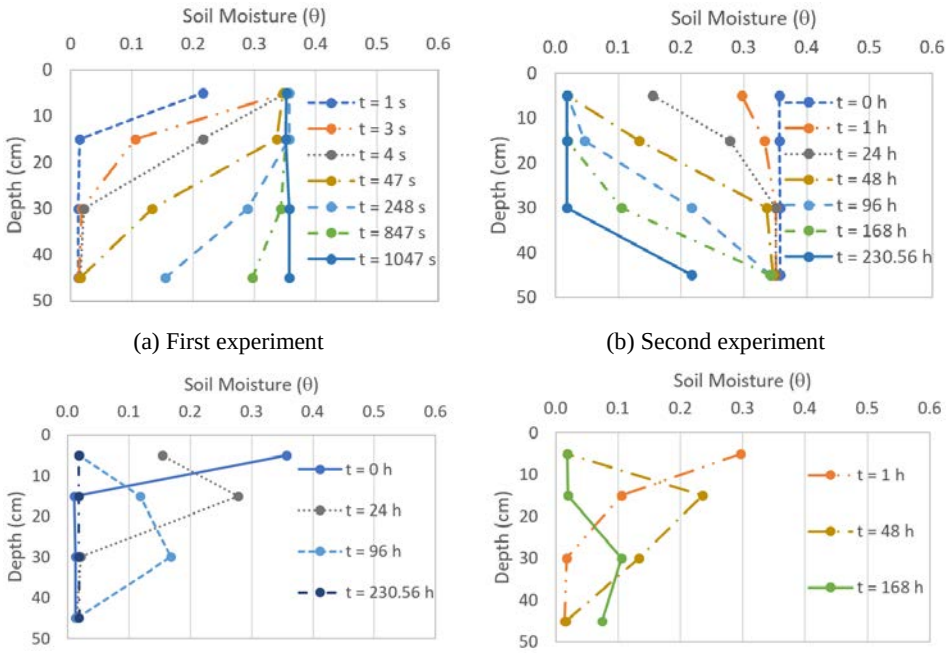

(a) First experiment

(b) Second experiment

(c) Third experiment: Readings at 0, 1 and 4 days (left), Readings at 1 h, 2 days and 1 week(right)

Figure 7 Variation of soil moisture.

The patterns of the downward water movement, in the first experiment, represented the infiltration phenomenon, while the upward water movement, in the second experiment, represented the evaporation process. The patterns of wetting and drying fronts in the first and second experiments are shown in Figures 7(a) and (b). They were fully saturated and fully dry at 1047 s and 230 h, respectively, due to the saturated water content at 0.360. The pattern of simultaneous downward and upward water movement in the third experiment represented the phenomenon of infiltration under free-draining conditions with

separate water-drop flux. The simultaneous-front patterns are shown in Figure 7(c). Long-term water movement inside the bare soil was clearly observed in the 3-day and 1-week experiments, where the soil moisture amount was greater than the residual water content. In this context, the superposition model of both water-ponding orientations is based on driving forces from both hydraulic gradients and thermal gradients. The third experiment showed the movement of optimum water-content over time among the water-content distribution inside the bare soil. The optimum water content declined while under heat conduction from the light bulb.

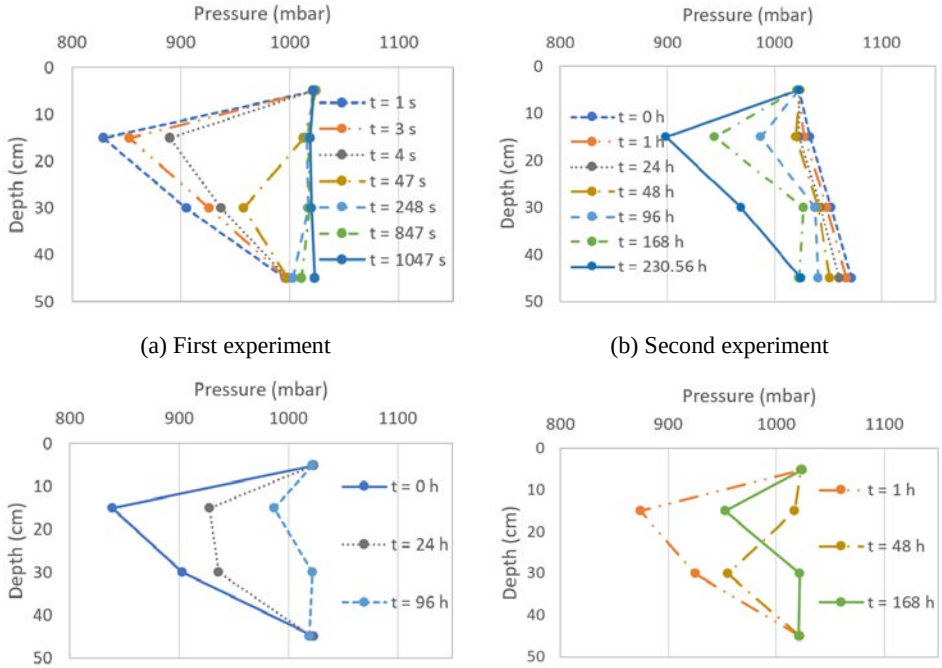

(a) First experiment

(b) Second experiment

(c) Third experiment: Readings at 0, 1 and 4 days (left), Readings at 1 h, 2 days and 1 week (right)

Figure 8 Variation of pressure.

Pressure variation in each experiment was measured according to the water-movement patterns. Low-pressure areas (less than 1 atmospheric pressure), which declined and inclined with depth, are shown in Figures 8(a) and (b). The pressure variation in the third experiment represented both previous conditions (see Figure 8(c)), where the potential of the low-pressure area was relatively reserved. Long-term pressure variation inside the bare soil was clearly observed in the 3-day and 1-week experiments (Figure 8(c)). There was no change at a pressure measurement depth of 5 cm, where the soil surface was slightly ponded

due to the saturated condition close to the top of the porous media in the first and third experiments. Meanwhile, there was free pressure that was only affected by atmospheric pressure in the second experiment. The pressure amount was then read equal to the atmospheric pressure. In this case, the pressure sensor basically captured the accumulation values of internal pore pressure and surface pressure (or free pressure). However, the pressure sensor at 5 cm of depth did not work properly during the experiments.

Temperature variation in the second and third experiments showed identical measurement patterns. This was caused by heat conduction affected by the light bulb with the same elapsed time. A dramatic increase in temperature was shown by the upper sensors, which indicates a fast heat propagation at the bare soil surface. Conversely, a low temperature (close to 30 degrees) occurred in the position of the other layers. This indicates that the heat was not affected at the bottom of the layer in the 1-week experiment. The temperature variation is shown in Figure 9.

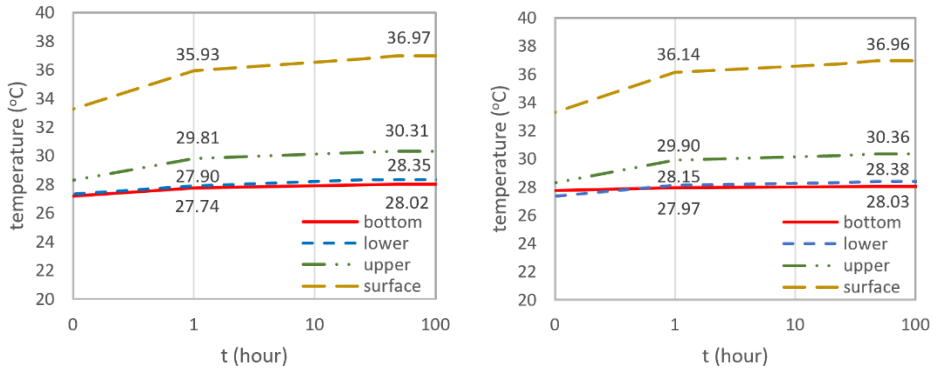

(a) Second experiment (b) Third experiment

Figure 9 Variation of temperature

3.3 Instrument Improvement

Calibration was performed before the experiments to meet quality requirements. Replacement of all sensors was required to ensure their resistivity and durability. The improvements were specifically related to the sensor stick, the tube arrangement and the substitution type. The configurations of the instrument improvements are shown in Figure 10. The stick was modified from porous to massive to minimize air escape during the infiltration process (Figure 10(a)). The tube arrangement for the pressure sensor was minimized to a more representative condition of porous media (Figure 10(b)), while the air pressure measurement was done by detecting the variation of air pressure inside the modified outer tube around the soil sample.

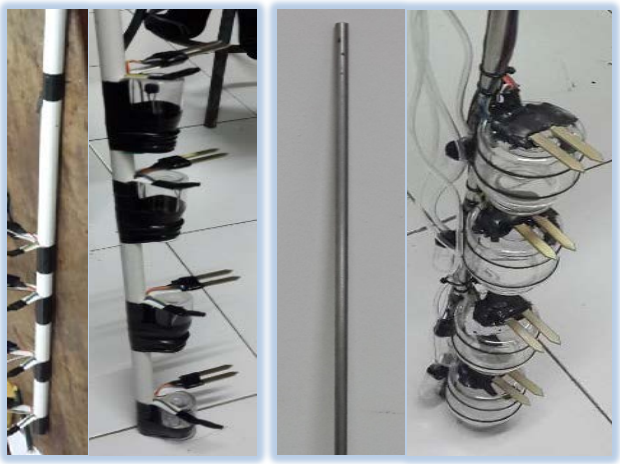

(a) Sensor stick modification: Previous stick (left), Modified stick (right)

(b) Tube arrangement: Previous tube and module (left), modified tube (center), pressure calibration (right)

(c) Moisture sensor substitution

Figure 10 Instrument improvements.

The resistance-based soil moisture sensor was substituted with a capacitance-based sensor for the second and third experiments due to the final elapsed time for each simulation. The soil moisture sensor of the second type is better for

long-term observation in the apparatus. The difference in durability of the two types of sensors can be seen from their 1-week usage, as shown in Figure 10(c).

4 Conclusion

Measurements of water movement in a soil-column apparatus were carried out successfully in a multistage experiment with known pressure and temperature values. Some instruments were modified and showed better results in comparison with the initial instrument setup. The use of sensors, tubes and sticks was configured differently at each stage of the experiment.

The initiation of the primary shape of each pattern of the wetting-front, drying-front and simultaneous-front schemes was established, while the third pattern produced a new shape for the study of infiltration under free-draining conditions. This shape refines the conventional wetting-front shape that was previously introduced by the Green-Ampt theory.

Acknowledgements

The authors would like to thank the Institute of Research and Community Services (LPPM) of Bandung Institute of Technology for the P3MI research funding. We are also grateful to Mr. Akub and the instrumentation teams at the Earth Physics and Complex-system laboratory for the technical assistance.

References

[1] Banimahd, S.A. & Zand, S., *Simulation of Evaporation, Coupled Liquid Water, Water Vapor and Heat Transport through the Soil Medium*, Agricultural Water Management, **130**, pp. 168-177, 2013.

[2] Green, W.H. & Ampt, G.A., *Studies on Soil Physics I. The Flow of Air and Water through Soils*, Journal of Agricultural Research, **4**, pp. 1-24, 1911.

[3] Gowdish, L. & Muñoz-Carpena, R., *An Improved Green–ampt Infiltration and Redistribution Method for Uneven Multistorm Series*, Vadose Zone Journal, **8**(2), pp. 470-479, 2009.

[4] Guymon, G-L., *Unsaturated Zone Hydrology*, Englewood Cliffs, NJ, United States: PTR Prentice Hall, 1994.

[5] Hayek, M., *Water Pulse Migration through Semi-infinite Vertical Unsaturated Porous Column with Special Relative-Permeability Functions: Exact Solutions*, Journal of Hydrology, **517**, pp. 668-676, 2014.

[6] Grifoll, J., Gastó, J.M. & Cohen, Y., *Non-Isothermal Soil Water Transport and Evaporation*, Advances in Water Resources, **28**(11), pp. 1254-1266, 2005.
[7] Herrada, M.A., Gutiérrez-Martin, A. & Montanero, J.M., *Modeling Infiltration Rates in a Saturated/Unsaturated Soil Under the Free Draining Condition*, Journal of Hydrology, **515**, pp. 10-15, 2014.
[8] Richards, L.A., *Capillary Conduction of Liquids through Porous Mediums*, Physics, **1**(5), pp. 318-333, 1931.
[9] Ma, Y., Feng, S., Su, D., Gao, G. & Huo, Z., *Modeling Water Infiltration in a Large Layered Soil Column with a Modified Green-ampt Model and HYDRUS-1D*, Computers and Electronics in Agriculture, **71**, pp. 40-47, 2010.
[10] Mao, L., Li, Y., Hao, W., Zhou, X., Xu, C. & Lei, T., *A New Method to Estimate Soil Water Infiltration Based on a Modified Green-ampt Model*, Soil and Tillage Research, **161**, pp. 31-37, 2016.
[11] Mein, R.G. & Larson, C.L., *Modeling Infiltration during Steady Rain*, Water Resources Research, **9**, pp. 384-394, 1973.
[12] Miracapillo, C. & Morel-Seytoux, H., *A Numerical Experiment to Determine the Soil Water Contents in the Unsaturated Zone and the Water Table Response under Transient Ponding Conditions*, Procedia Environmental Sciences, **25**, pp. 150-157, Jan. 2015.
[13] Mohammadzadeh-Habili, J. & Heidarpour, M., *Application of the Green-Ampt Model for Infiltration into Layered Soils*, Journal of Hydrology, **527**, pp. 824-832, 2015.
[14] Rawls, W.J., Brakensiek, D.L., Simanton, J.R. & Kohl, K.D., *Of a Crust Factor for a Green-ampt Model*, Transactions of the ASAE, **33**, Jul. 1990.
[15] Siemens, G. & Bathurst, R., *Numerical Parametric Investigation of Infiltration in One-Dimensional Sand-Geotextile Columns*, Geotextiles and Geomembranes, **20**, pp. 460-474, 2010.
[16] Suttisong, S., Rattanadecho, P. & Montienthong, P., *Comparison of Stefan Model with Single-Phase Model of Water Infiltration Process in Unsaturated Porous Media (Theory and Experiment)*, Journal of Hydrology, **497**, pp. 145-151, 2013.
[17] Voller, V.R., *On a Fractional Derivative Form of the Green-ampt Infiltration Model*, Advances in Water Resources, **34**(2), pp. 257-262, 2011.
[18] Zhang, W., Zhang, Z. & Wang, K., *Experimental Study and Simulations of Infiltration in Evapotranspiration Landfill Covers*, Water Science and Engineering, **2**(3), pp. 96-109, 2009.
[19] Hendrayanto, Kosugi, K. & Mizu, T., *Field Determination of Unsaturated Hydraulic Conductivity of Forest Soils*, Journal of Forestry, **3**, pp. 11-17, 1998.

[20] Ibrahim, A., Mukhlisin, M. & Jaafar, O., *Rainfall Infiltration through Unsaturated Layered Soil Column*, Sains Malaysiana, **43**(10), pp. 1477-1484, 2014.

[21] Kapetas, L., Dror, I. & Berkowitz, B., *Evidence of Preferential Path Formation and Path Memory Effect During Successive Infiltration and Drainage Cycles in Uniform Sand Columns*, Journal of Contaminant Hydrology, **165**, pp. 1-10, 2014.

[22] Lee, M., Lee, L., Kassim, A. & Gofar, N., *Performances of Two Instrumented Laboratory Models for the Study of Rainfall Infiltration into Unsaturated Soils*, Engineering Geology, **117**, 2010.

[23] Swartzendruber, D., *Derivation of a Two-term Infiltration Equation from the Green-Ampt Model*, Journal of Hydrology, **236**(3), pp. 247-251, 2000.

[24] Mellouli, H., Wesemael, B., Poesen, J. & Hartmann, R., *Evaporation Losses from Bare Soils as Influenced by Cultivation Techniques in Semi-Arid Regions*, Agricultural Water Management, **42**, pp. 355-369, 2000.

[25] Menziani, M., Pugnaghi, S., Pilan, L., Santangelo, R. & Vincenzi, S., *Field Experiments to Study Evaporation from a Saturated Bare Soil*, Physics and Chemistry of the Earth, Part B: Hydrology, Oceans and Atmosphere, **24**(7), pp. 813-818, 1999.

[26] Price, J.S., Edwards, T.W.D., Yi, Y. & Whittington, P.N., *Physical and Isotopic Characterization of Evaporation from Sphagnum Moss*, Journal of Hydrology, **369**(1), pp. 175-182, 2009.

[27] Raziyeh, A., Mehdi, H. & Mohammad, B., *Simulating Unsteady Soil Evaporation Under Variable Water Content Based on Campbell's Two-Parameter Retention Model*, **1**(4), pp. 87-97, 2012.

[28] Saito, H., Šimůnek, J. & Mohanty, B.P., *Numerical Analysis of Coupled Water, Vapor, and Heat Transport in the Vadose Zone*, Vadose Zone Journal, **5**(2), pp. 784-800, 2006.

[29] Zhang, J., Chen, Q. & You, C., *Numerical Simulation of Mass and Heat Transfer Between Biochar and Sandy Soil*, International Journal of Heat and Mass Transfer, **91**, pp. 119-126, 2015.

[30] Huang, R.Q. & Wu, L.Z., *Analytical Solutions to 1-D Horizontal and Vertical Water Infiltration in Saturated/Unsaturated Soils Considering Time-varying Rainfall*, Computers and Geotechnics, **39**, pp. 66-72, 2012.

[31] Nowamooz, H., Nikoosokhan, S., Lin, J. & Chazallon, C., *Finite Difference Modeling of Heat Distribution in Multilayer Soils with Time-spatial Hydrothermal Properties*, Renewable Energy, **76**, pp. 7-15, 2015.

[32] Sadeghi, M., Tuller, M., Gohardoust, M.R. & Jones, S.B., *Column-scale Unsaturated Hydraulic Conductivity Estimates in Coarse-textured Homogeneous and Layered Soils Derived under Steady-State Evaporation from a Water Table*, Journal of Hydrology, **519**, pp. 1238-1248, 2014.

[33] Mander, G. & Arora, M., *Design of Capacitive Sensor for Monitoring Moisture Content of Soil and Analysis of Analog Voltage with Variability in Moisture*, in 2014 Recent Advances in Engineering and Computational Sciences, RAECS 2014, pp. 1-5, 2014.

[34] Saleh, M., Elhajj, I., Asmar, D., Bashour, I. & Kidess, S., *Experimental Evaluation of Low-cost Resistive Soil Moisture Sensors*, presented at the International Multidisciplinary Conference on Engineering Technology (IMCET), pp. 179-184, 2016.

[35] Jr, C.H.R. & Kinney, L.L., *Fundamentals of Logic Design*, 6th ed. Stamford, CT: Cengage Learning, 2009.

[36] CD4051BMT Datasheet Texas Instruments CD4051B CMOS Single 8-Channel Analog Multiplexer/Demultiplexer with Logic-Level Conversion Engineering360, Available at: https://datasheets. globalspec.com/ds/3611/ TexasInstruments/C07DEB36-6430-4F56-8F7E-025FB61EEED2. (26-May 2018)

[37] Hakam, A., *Laboratory Liquefaction Test of Sand Based on Grain Size and Relative Density*, Journal of Engineering and Technological Sciences, **48**(3), pp. 334-344, 2016.